Granular Pressure in a Liquid-Fluidized Bed as Revealed by Diffusing Wave Spectroscopy

V. Zivkovic and M. J. Biggs
School of Chemical Engineering, The University of Adelaide, Adelaide, SA 5005, Australia

D. Glass
Institute for Materials and Processes, The University of Edinburgh, Sanderson Building, King's Buildings, Mayfield Road, Edinburgh EH9 3JL, U.K.

DOI 10.1002/aic.12650
Published online May 6, 2011 in Wiley Online Library (wileyonlinelibrary.com).

The granular pressure and granular temperature underpin various models of granular flows while they are playing an increasing role in modeling of other phenomena in granular systems such as heat transfer, segregation, erosion, attrition, and aggregation. The development and validation of these theories demand experimental determination of these two quantities. Diffusing wave spectroscopy (DWS) is now an accepted technique for measurement of granular temperature in dense granular systems. Using granular temperature data obtained from DWS with the kinetic theory of granular flow, we have derived the granular pressure data for a liquid-fluidized bed. The determined variation of the mean bed granular pressure with mean bed solid volume fraction compares favorably with previously published experimental data and theoretical models of others. Where discrepancies do occur, they may be attributed to differences in particle inertia, suggesting further work on granular pressure models is required. Finally, we report the variation of the granular pressure with height above the distributor for several mean solids volume fractions. © 2011 American Institute of Chemical Engineers *AIChE J,* 58: 1069–1075, 2012

Keywords: fluidization, granular materials, granular pressure, multiphase flow, particle, diffusing wave spectroscopy

Introduction

Collisional particle pressure, or granular pressure, is defined as the force exerted by a moving granular medium on the walls of the vessel containing the medium.[1,2] The particle pressure underpins various granular flow models[3,4] and is a dominant factor determining the stability of the flow in fluidized beds.[5–7]

Campbell and Wang[1] developed a probe to isolate the particle pressure in a fluidized bed by taking the difference between the total and the fluid pressure exerted at the point of measurement. This particle pressure transducer is very simple and consists of a solid diaphragm flush-mounted into the bed wall. The face of the diaphragm experiences the combined pressure of fluid and particles, whereas the rear experiences only fluid forces as particles are prevented from entering through the access holes into a chamber behind the diaphragm. Campbell and collaborators[1,8,9] and others[10–12] measured the particle pressure in gas-fluidized beds using this approach. A second more recent approach relies on a high-frequency-response pressure transducer that detects changes in pressure lasting up to 2 μs,[2] enabling the measurement of particle pressure from individual particle impacts without the interference from the fluid-related pressure.[2,13] This approach has been used to measure particle pressure in liquid,[2] gas-liquid,[13] and vibrated[14] fluidized

Correspondence concerning this article should be addressed to V. Zivkovic at vladimir.zivkovic@adelaide.edu.au

beds. A third yet unexploited approach of obtaining the particle pressure experimental data is to "turn on its head," the approach used by Polashenski and Chen[10] to determine granular temperature from experimentally granular pressure; i.e., use constitutive relations from the kinetic theory of granular flow with experimentally determined granular temperature to compute the granular pressure.

Liquid-fluidized beds usually expand in homogenous way in contrast to gas-fluidized beds, which are generally unstable and give rise to bubbling behavior. This makes liquid-fluidized beds particularly suitable for testing two-phase flow models across a wide range of solid fractions.[15] Yet, there has been only one experimental study of the particle pressure in liquid-fluidized bed.[2] Zenit et al.[2] study was very thorough, but they were using relatively large and heavy glass or steel particles which fall in the transitional or even bubbling regime of the flow map[16] based on the criterion equation of Gibilaro et al.[17] Even though it was not reported by Zenit et al.,[2] nonhomogenous behavior and even the appearance of bubbles can be expected in the transitional regime of liquid fluidization, which in principle can have an influence on the particle pressure. Hence, it is desirable to obtain granular pressure measurement for smaller particles, which strictly fall in the homogenous regime of liquid fluidization—this is done here.

We report here the granular pressure data for a thin, rectangular bed of small glass particles fluidized by water across a wide range of superficial velocities and, hence, bed solids fraction. The granular pressure was determined by using the granular temperature data obtained from diffusing wave spectroscopy (DWS)[18] in expressions for the pressure derived from the kinetic theory of granular flow.[19,20] We first outline the experimental details, including an overview of DWS and details pertaining to the apparatus and the particulate material, and the experimental procedure used. This is followed by presentation of the results obtained and their discussion.

Experimental Details

Experimental apparatus

The fluidized bed apparatus is illustrated in Figure 1a. The main part is a half-meter high-rectangular bed with a cross-section of 200 mm by 20 mm. It was mounted on a linear stage so that different points of the bed could be investigated with ease. The distributor, which consists of a stainless steel mesh of 40-μm apertures and a 5-cm deep-packed bed of 1.5-mm stainless steel beads, was designed to provide highly uniform and homogeneous fluidization. The overflow water at the top of the column was recirculated back into a feed reservoir and a centrifugal pump, forming a closed loop. The liquid flow was measured by a calibrated rotameter (KDG 2000, KDG instruments, UK) and temperature of water was maintained at 20 ± 0.5°C. The fluidized particles were small glass particles with density of $\rho_p = 2500$ kg/m^3 (SiLibeads type S, Sigmund Lindner, UK). The beads were carefully resieved between two close meshes to obtain narrowly distributed glass beads of diameter $d_p = 165 \pm 15$ μm. The liquid fluidized bed was filled with granular material to give a 75-mm defluidized-bed height.

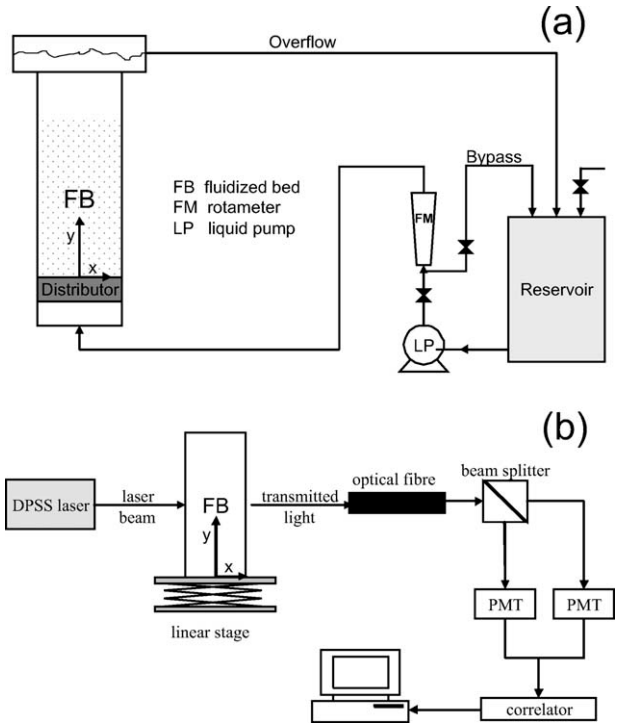

Figure 1. Schematic diagram of (a) liquid FB apparatus and (b) DWS apparatus.

DWS, which is described in detail by Weitz and Pine,[21] is a multiple light scattering technique with high spatiotemporal resolution (1–10 nm, 2 ns). It has been applied in the study of particle dynamics in various dense granular systems (see, e.g.,[22,23] and references therein). The DWS apparatus for use here in the transmission mode is illustrated in Figure 1b. A 400-mW diode pumped solid state linearly polarized laser (Torus 532, Laser Quantum, Cheshire, UK) operating at a wavelength of $\lambda = 532$ nm in single longitudinal mode illuminates one side of the bed at the point of interest with an ~2-mm diameter laser beam. The light passes through the medium, scattering many times before exiting the back of the bed as a diffuse spot of ~20 mm diameter for our bed of 20 mm thickness. The scattered light was collected over time, t, with a single mode optical fiber (OZ Optics, Ottawa, Canada). The collected light signal was bifurcated and the 50/50 split light signal fed into two matched photomultiplier tubes (PMTs) to reduce spurious correlations due to possible after-pulsing effects of the detector. The intensity outputs $I(t)$ from the PMTs were amplified and fed to a multitau digital correlator (Flex 05, Correlator.com), which performed a pseudo cross-correlation analysis in real time to give the intensity autocorrelation function (IACF), $g_2(t)$, that was stored on a personal computer for further offline analysis as detailed below.

Experimental Procedure

Measurements of solid volume fraction

In a steady-state regime of fluidization, the height of the front between fluidized particles and clear fluid at the top of the bed was determined. The height was measured using a measuring tape glued to the side bars of the apparatus with

an accuracy of ±1 mm. By measuring the mean fluidized-bed height, h, the mean solids volume fraction of the bed, $<\phi>$, was then calculated by

$$\langle \phi \rangle = \frac{m_p}{\rho_p A h} \tag{1}$$

where m_p is the mass of fluidized particles, and A is the cross-sectional area.

The solids volume fraction was also determined as a function of height above the bed distributor, y, by measuring the transmitted laser light intensity through the liquid-fluidized bed normalized to transmission through a reference sample of the same thickness, I/I_r[24–26]. The light intensity was detected and recorded with a digital optical power meter (Model 815, Newport Corporation). The signals were averaged over 60 s, a time much larger than the expected period of any density waves. For calibration, we used height averaged values of the transmitted light intensities[24] at a fixed mean particle solids volume fraction as it gave slightly better results than mid-height transmitted light intensities, an approach used by Segre and McClymer.[25]

Measurement of granular temperature

A detailed description of the method used to determine the granular temperature in the liquid-fluidized bed using DWS is provided in Zivkovic et al.[18] We provide here, however, a brief overview. IACFs were obtained by collecting and correlating 10 blocks of data of 30 s each. Each IACF was then subject to further analysis as follows. The normalized electric-field autocorrelation function (FACF), $g_1(t)$, was obtained from the IACF, $g_2(t)$, using the Siegert relationship.[21,27]

$$g_2(t) \equiv \frac{\langle I(0)I(t)\rangle}{\langle I\rangle^2} = 1 + \beta_1 |g_1(t)|^2 \tag{2}$$

where β_1 is a phenomenological parameter determined from the intercept of the IACF; this phenomenological parameter was always found to be $\beta_1 \approx 0.5$, as expected. The mean square displacement (MSD) of the particles, $\langle \Delta r^2(t)\rangle$, was determined by inverting the FACF using the formula given by Weitz and Pine[21]

$$g_1(t) = \frac{\frac{L/l^*+4/3}{z_0/l^*+2/3}\left[\sinh\left(\frac{z_0}{l^*}\sqrt{X}\right) + \frac{2}{3}\sqrt{X}\cosh\left(\frac{z_0}{l^*}\sqrt{X}\right)\right]}{\left(1+\frac{4}{9}X\right)\sinh\left(\frac{L}{l^*}\sqrt{X}\right) + \frac{4}{3}\sqrt{X}\cosh\left(\frac{L}{l^*}\sqrt{X}\right)}; \quad X = \langle \Delta r^2(t)\rangle k_0^2 + \frac{3l^*}{l_a} \tag{3}$$

where L is the sample thickness (20 mm here), l^* is the transport mean free path, l_a is the absorption path length, $z_0 = \gamma l^*$ is the distance over which the incident light is randomized, and $k_0 = 2\pi/\lambda$ is wave vector of light in the medium. The scaling factor, γ, was set to unity in line with common practice.[21,28]

The square of particle velocity fluctuations about the mean flow velocity can be derived straightforwardly from the ballistic region of the MSD,[29] provided it is resolved, where

$$\langle \Delta r^2 \rangle = \langle \delta v^2 \rangle t^2 \tag{4}$$

The granular temperature for a three-dimensional flowing granular material is defined as

$$\theta = \frac{1}{3}\langle \delta v^2 \rangle \tag{5}$$

Equation 3 requires knowledge of the transport mean free path, l^*, or step size in the random walk of photons, and the diffusive absorption path length, l_a, which accounts for light absorption, at the positions and conditions considered. They were determined using the method of static transmission[21,30] as a function of solid volume fraction and height above the distributor.[18]

A second decay in the IACF was observed at time scales of order 0.1 s (see, e.g., Figure 5a in Zivkovic et al.[18]), which is consistent with the frequency of density waves in homogeneous fluidization (i.e., 4–8 Hz[31]). As this timescale is far greater than that associated with the granular temperature determination (i.e., 1–10 μs),[18] the granular temperature measured here is unrelated to the oscillatory motion associated with the density waves.

Determination of granular pressure

For determination of the granular pressure given the granular temperature, we used the kinetic theory of granular flow expression[19,20]

$$P^* = \rho_p \phi \theta [1 + 2\phi g_0(\phi)(1+e)] \tag{6}$$

where $g_0(\phi)$ is the radial distribution function (RDF) of the particles, and e is the restitution coefficient. We determined the granular pressure using three common forms of the RDF, namely, those proposed by Bagnold[32]

$$g_0(\phi) = \left[1 - (\phi/\phi_{max})^{1/3}\right]^{-1} \tag{7}$$

Carnahan and Starling,[33]

$$g_0(\phi) = \frac{2-\phi}{2(1-\phi)^3} \tag{8}$$

and Lun and Savage,[34]

$$g_0(\phi) = (1 - \phi/\phi_{max})^{-5\phi_{max}/2} \tag{9}$$

where ϕ_{max} is the maximum possible solid volume fraction of the system, which was assumed here to be equal to the random close packing limit of 0.64.

Defining a coefficient of restitution, e, in a liquid-fluidized bed is problematic as the interparticle collisions will invariably be mediated by a liquid film. Some[35] have, however, suggested use of an "effective" restitution coefficient that takes into account energy dissipation due to the lubrication effect arising from the thin liquid film that will exist between colliding particles in liquid-fluidized systems, whereas others have adopted this concept in practise.[15,31,37,38] On the basis of their experiments, Gidaspow and Huilin[35] suggest a value for e very close to 1, and this value has been used in simulation.[36] However, more often a coefficient of restitution of less than one, usually 0.9, has

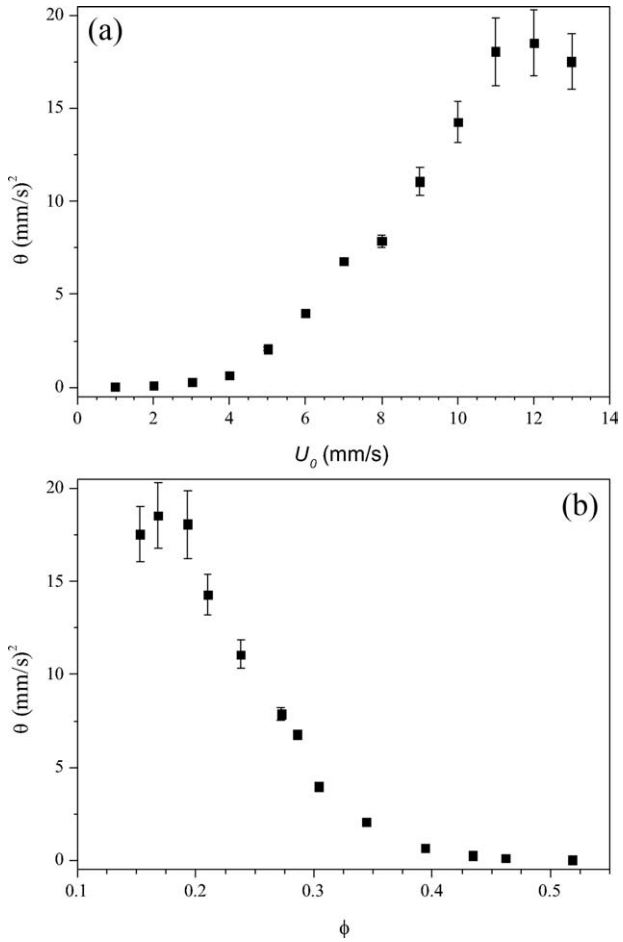

Figure 2. The variation of height averaged values of granular temperature, θ, with superficial velocity U_0 (a) and with the mean bed solid volume fraction, $\langle\phi\rangle$ (b).

Error bars are standard deviation of height averaged granular temperature data.

been used in simulation studies.[15,31,37,38] A sensitivity analysis of our result indicates that the granular temperature varies by around 4% as the coefficient of restitution is varied from 0.9 to 1. We, therefore, have used $e = 0.95$, which actually happens to correspond to the dry coefficient of restitution as another utilized approximation.[39]

Results and Discussion

Granular temperature variation with superficial velocity and solid volume fraction

Figure 2a shows variation of height averaged granular temperature with superficial velocity. The granular temperature increases with superficial velocity up to a maximum at $U_0 = 7.5$ mm/s. To explain the observed maximum, we replot the data to obtain the variation with the mean solid fraction, $\langle\phi\rangle$, as shown in Figure 2b. This exhibits a maximum at $\langle\phi\rangle = 0.175$. This is in line with the simulations of Gevrin et al.,[15] who reported a maximum in the granular temperature of glass particles at a solid fraction close to $\phi = 0.2$. A similar trend was observed when the local solid fraction was plotted against the local velocity fluctuation data,[18] indicating that the granular temperature may be described solely in terms of the solids volume fraction, ϕ, for liquid-fluidized beds.

Granular pressure variation with superficial velocity and solid volume fraction

The calculated values of the granular pressure using the kinetic theory of granular flow model expressions are strongly affected by the choice of RDF. Gidaspow and Huilin[35,40] determined experimentally the RDF in a rectangular liquid-fluidized bed and found that it lies between the Bagnold form, Eq. 7, and that of Carnahan and Starling, Eq. 8. It is reasonable to assume that is the case here given the similarities of our system to that of Gidaspow and Huilin. While in the most simulation studies, the Bagnold expression is used,[31,37,38] Gevrin et al.[15] used that of Lun and Savage, Eq. 9, in their simulation work, which is the reason, we included consideration of this RDF here as well.

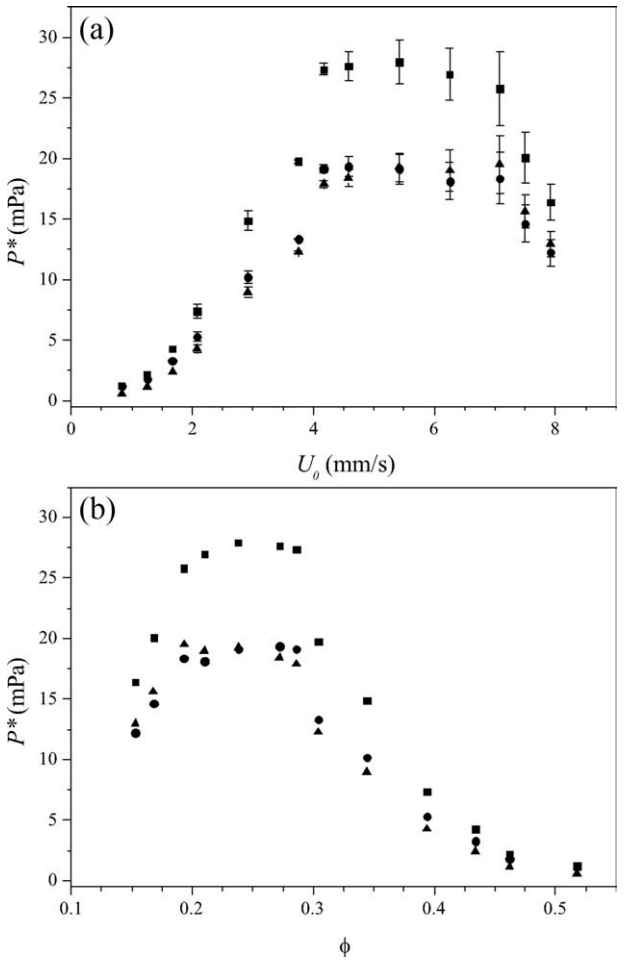

Figure 3. Variation of mean granular pressure, P^*, with: (a) superficial velocity U_0; and (b) mean bed solids volume fraction, $\langle\phi\rangle$.

The data has been obtained from Eq. 6 using the radial distribution functions proposed by Bagnold (square), Carnahan and Stirling (triangle), and Lun and Savage (circles). Error bars are standard deviation of height averaged granular pressure data (not shown on plot (b) for clarity).

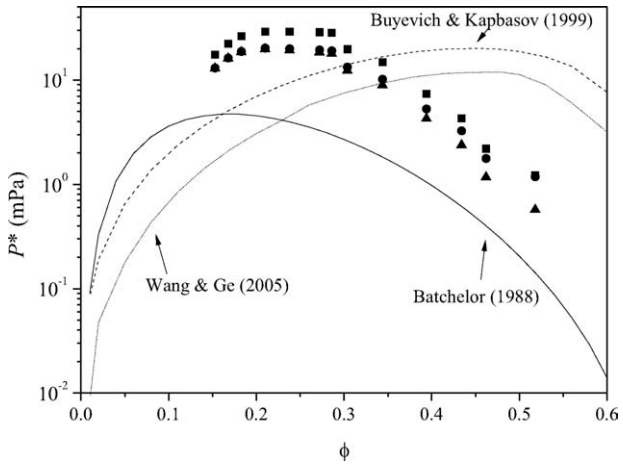

Figure 4. Comparison of the experimental results (points) with theoretical models of Batchelor,[7] Buyevich and Kapbasov,[41] and Wang and Ge.[39]

Symbols representing the experimental data are as for Figure 3.

Experimental data shown in Figure 2b was used to calculate the mean granular pressure in the bed using Eq. 6 with the three different forms of RDF, Eqs. 7–9. Note that the magnitude of the determined granular pressure is order of mPa, which will make very difficult, if not impossible, to measure it using pressure transducer approaches described in the Introduction. Figure 3a, which shows the granular pressure variation with superficial velocity, indicates that while the granular pressure obtained from the Bagnold RDF is up to 50% larger than the granular pressure obtained using the other two RDF forms, the trends are very similar. In particular, irrespective of the RDF used, the granular pressure increases rapidly with superficial velocity until it plateaus for some intermediate range of velocities before decreasing as the superficial velocity approaches the particle terminal velocity. This is qualitatively very similar to the results of Zenit et al.,[2] especially for low inertia particles.

For better comparison, the granular pressure is plotted against the mean solids volume fraction as shown in Figure 3b. There is very little variation of the granular pressure with mean solids volume fraction in the maximum plateau region, but the mean granular pressure sharply decreases as

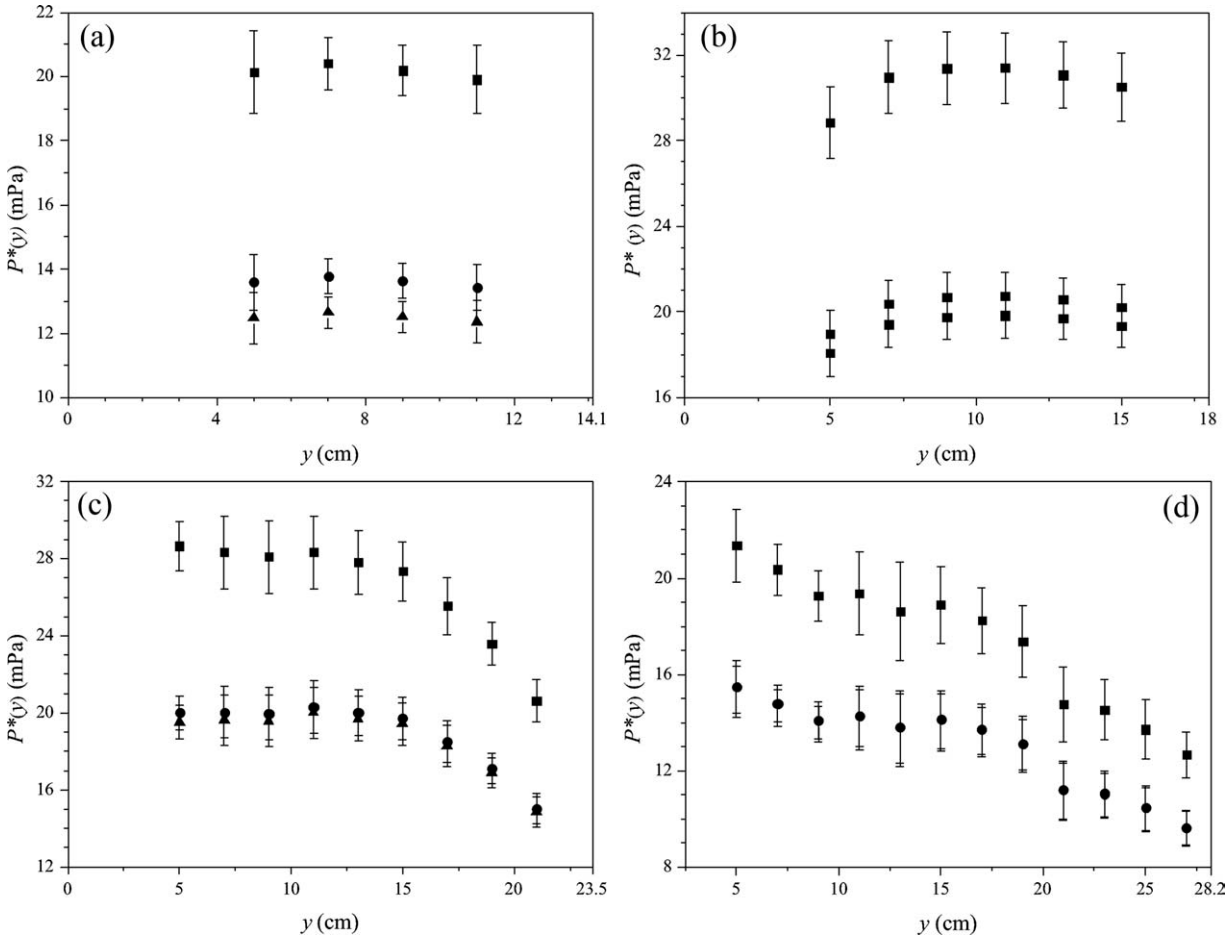

Figure 5. The local granular pressure, $P^*(y)$, as a function of the height above the distributor, y, for four mean bed solid volume fractions: (a) $\langle\phi\rangle = 0.306$, (b) $\langle\phi\rangle = 0.238$, (c) $\langle\phi\rangle = 0.183$, and (d) $\langle\phi\rangle = 0.153$.

The data has been obtained from Eq. 6 using the radial distribution functions proposed by Bagnold (square), Carnahan and Stirling (triangle), and Lun and Savage (circles). The right-hand borders of each plot represent the mean fluidized-bed heights, h. Error bars are standard deviation of calculated local granular pressure.

mean solids volume fraction approaches both the dilute and close-packed limits. The maximum granular pressure occurs at intermediate values of the mean solids volume fraction, between 0.2 and 0.3 in our case. This range is slightly lower than that of Zenit et al.,[2] who observed maxima at solid volume fractions between 0.3 and 0.35, but is in line with their observation that maximum pressure is located at lower solids volume fractions for smaller particles (i.e., low inertia particles).

Figure 4 compares the maximum particle pressures obtained here against the models proposed by Batchelor,[7] Buyevich and Kapbasov,[41] and Wang and Ge.[39] While the first of these models somewhat underpredicts the experimental results obtained here and presents a maximum at slightly lower solids volume fractions, its shape is otherwise remarkably similar. Both the models of Buyevich and Kapbasov[41] and Wang and Ge[39] predict a maximum in granular pressure for solid fraction of around 0.45, which is well above that obtained here but in line with that expected for high inertia particles for which they were tailored.[39] Moreover, the numerical results of the two-fluid model[15] are similar to these theoretical models, and accordingly show the greatest discrepancy with the experimental result for low inertia particles (e.g., nylon beads in the experimental work of Zenit et al.[2]). These results suggest that further work on models is still necessary to correctly capture the effect of particle inertia on granular pressure.

Spatial variation of granular pressure

We used the local solids volume fraction and granular temperature experimental data to obtain, for the first time as far as we are aware, the variation of the solids pressure in a liquid-fluidized bed with height above the distributor, Figure 5. Figures 5a, b show that the granular pressure varies little with height above the distributor for mean solids volume fractions above $\langle\phi\rangle = 0.238$. Near $\langle\phi\rangle = 0.238$, there appears to be a possibility of a weak variation of granular pressure with height, although the uncertainty in the experimental data means this variation is not unambiguous. This weak variation is perhaps not unexpected, as the mean solids volume fraction lies in the region where the granular pressure plateaus (cf., Figure 3b). Figures 5c, d show that for mean solids volume fractions below $\langle\phi\rangle = 0.238$, there is considerable variation of local particle pressure with height above the distributor. This confirms numerical results of Gevrin et al.[15] at low solids volume fractions.

Conclusions

Using the granular temperature measured by DWS with expressions from the kinetic theory of granular flow, we obtained a range of granular pressure data for 165-μm glass particles in a thin, rectangular water-fluidized bed. The derived mean bed granular pressure increases with mean bed solids fraction, until it plateaus at intermediate fractions (between 0.2 and 0.3) before decreasing again as the bed approaches the close packed limit. This is in line with experimental results of Zenit et al,[2] suggesting that the approach used here is suitable for obtaining granular pressure. The model of Batchelor[7] best describes trends of the experimental granular pressure data obtained here, whereas other models[39,41] are less suitable as they are for particles of higher inertia than considered here. The granular pressure was also found to vary significantly with height above the distributor at low mean bed solids volume fractions (i.e., at higher superficial velocities), in line with the numerical results of Gevrin et al.[15]

Literature Cited

1. Campbell CS, Wang DG. Particle pressure in gas-fluidized beds. *J Fluid Mech*. 1991;227:495–508.
2. Zenit R, Hunt ML, Brennen CE. Collisional particle pressure measurements in solid-liquid flows. *J Fluid Mech*. 1997;353:261–283.
3. Enwald H, Peirano E, Almstedt AE. Eulerian two-phase flow theory applied to fluidization. *Int J Multiphase Flow*. 1996;22:21–66.
4. Ishii M. *Thermo-Fluid Dynamic Theory of Two-phase Flow*. Paris: Eyrolles, 1975.
5. Needham DJ, Merkin JH. Propagation of a voidage disturbance in a uniformly fluidized bed. *J Fluid Mech*. 1983;131:427–454.
6. Foscolo PU, Gibilaro LG. Fluid dynamic stability of fluidised suspensions: the particle bed model. *Chem Eng Sci*. 1987;42:1489–1500.
7. Batchelor GK. A new theory of the instability of a uniform fluidized bed. *J Fluid Mech*. 1988;193:75–110.
8. Campbell CS, Rahman K. An improved particle pressure transducer. *Meas Sci Technol*. 1992;3:709–712.
9. Rahman K, Campbell CS. Particle pressures generated around bubbles in gas-fluidized beds. *J Fluid Mech*. 2002;455:103–127.
10. Polashenski W. Jr, Chen JC. Normal solid stress in fluidized beds. *Powder Technol*. 1997;90:13–23.
11. Gidaspow D, Huilin L. Equation of state and radial distribution functions of FCC particles in a CFB. *AIChE J*. 1998;44:279–291.
12. Polashenski W. Jr, Chen JC. Measurement of particle phase stresses in fast fluidized beds. *Ind Eng Chem Res*. 1999;38:705–713.
13. Buffière P, Moletta R. Collision frequency and collisional particle pressure in three-phase fluidized beds. *Chem Eng Sci*. 2000;55:5555–5563.
14. Falcon E, Aumaitre S, Evesque P, Palencia F, Lecoutre-Chabot C, Fauve S, Beysens D, Garrabos Y. Collision statistics in a dilute granular gas fluidized by vibrations in low gravity. *Europhys Lett*. 2006;74:830–836.
15. Gevrin F, Masbernat O, Simonin O. Granular pressure and particle velocity fluctuations prediction in liquid fluidized beds. *Chem Eng Sci*. 2008;63:2450–2464.
16. Di Felice R. Hydrodynamics of liquid fluidisation. *Chem Eng Sci*. 1995;50:1213–1245.
17. Gibilaro LG, Di Felice R, Foscolo PU. Added mass effects in fluidized beds: application of the Geurst-Wallis analysis of inertial coupling in two-phase flow. *Chem Eng Sci*. 1990;45:1561–1565.
18. Zivkovic V, Biggs MJ, Glass DH, Pagliai P, Buts A. Granular temperature in a liquid fluidized bed as revealed by diffusing wave spectroscopy. *Chem Eng Sci*. 2009;64:1102–1110.
19. Gidaspow D. *Multiphase Flow and Fluidization—Continuum and Kinetic Theory Descriptions*. San Diego: Academic Press, 1994.
20. Jackson R. *The Dynamics of Fluidized Beds*. New York: Cambridge University Press, 2000.
21. Weitz DA, Pine DJ. *Diffusing-wave spectroscopy*. In: Brown W, editor. *Dynamic Light Scattering: The Method and Some Applications*. Oxford: Clarendon Press, 1993:652–720.
22. Zivkovic V, Biggs MJ, Glass DH, Xie L. Particle dynamics and granular temperatures in dense fluidized beds as revealed by diffusing wave spectroscopy. *Adv Powder Technol*. 2009;20:227–233.
23. Kim K, Pak HK. Diffusing-wave spectroscopy study of microscopic dynamics of three-dimensional granular systems. *Soft Matter*. 2010;6:2894–2900.
24. Duru P, Nicolas M, Hinch J, Guazzelli É. Constitutive laws in liquid-fluidized beds. *J Fluid Mech*. 2002;452:371–404.
25. Segrè PN, McClymer JP. Fluctuations, stratification and stability in a liquid fluidized bed at low Reynolds number. *J Phys Condens Matter*. 2004;16:S4219–S4230.
26. Tee SY, Mucha PJ, Brenner MP, Weitz DA. Velocity fluctuations in a low-Reynolds-number fluidized bed. *J Fluid Mech*. 2008;596:467–475.

27. Berne JB, Pecora R. *Dynamic Light Scattering*. New York: Wiley-Interscience Publication, 1976.
28. Xie L, Biggs MJ, Glass D, McLeod AS, Egelhaaf SU, Petekidis G. Granular temperature distribution in a gas fluidized bed of hollow microparticles prior to onset of bubbling. *Europhys Lett*. 2006;74: 268–274.
29. Menon N, Durian DJ. Diffusing-wave spectroscopy of dynamics in a three-dimensional granular flow. *Science*. 1997;275:1920–1922.
30. Leutz W, Rička J. On light propagation through glass bead packings. *Opt Commun*. 1996;126:260–268.
31. Lettieri P, Di Felice R, Pacciani R, Owoyemi O. CFD modelling of liquid fluidized beds in slugging mode. *Powder Technol*. 2006;167: 94–103.
32. Bagnold RA. Experiments on a gravity-free dispersion of large solid spheres in a Newtonian fluid under shear. *Proc R Soc London Ser A*. 1954;225:49–63.
33. Carnahan NF, Starling KE. Equation of state for nonattracting rigid spheres. *J Chem Phys*. 1969;51:635–636.
34. Lun C, Savage S. The effects of an impact velocity dependent coefficient of restitution on stresses developed by sheared granular materials. *Acta Mech*. 1986;63:15–44.
35. Gidaspow D, Huilin L. A comparison of gas-solid and liquid-solid fluidization using kinetic theory and statistical mechanics. *Fluidization IX*. 1998:661–668.
36. Cheng Y, Zhu JX. CFD modelling and simulation of hydrodynamics in liquid-solid circulating fluidized beds. *Can J Chem Eng*. 2005;83: 177–185.
37. Cornelissen JT, Taghipour F, Escudié R, Ellis N, Grace JR. CFD modelling of a liquid-solid fluidized bed. *Chem Eng Sci*. 2007;62: 6334–6348.
38. Wang S, Li X, Wu Y, Li X, Dong Q, Yao C. Simulation of flow behavior of particles in a liquid–solid fluidized bed. *Ind Eng Chem Res*. 2010;49:10116–10124.
39. Wang J, Ge W. Collisional particle-phase pressure in particle-fluid flows at high particle inertia. *Phys Fluids*. 2005;17:1–3.
40. Gidaspow D, Huilin L. Liquid-solid fluidization using kinetic theory. *AIChE Symposium Series No. 317*. 1997;93:12–17.
41. Buyevich YA, Kapbasov SK. Particulate pressure in disperse flow. *Int J Fluid Mech Res*. 1999;26:72–97.

Manuscript received Oct. 19, 2010, revision received Feb. 22, 2011, and final revision received Apr. 4, 2011.